ACMTF for Fusion of Multi-Modal Neuroimaging Data and Identification of Biomarkers

Evrim Acar*, Yuri Levin-Schwartz†, Vince D. Calhoun‡§ and Tülay Adalı†
*Faculty of Science, University of Copenhagen, DK-1958 Frederiksberg, Denmark, Email: evrim@life.ku.dk
†Department of Computer Science and Electrical Engineering, University of Maryland Baltimore County, Baltimore, MD
Email: adali@umbc.edu, ylevins1@umbc.edu
§The Mind Research Network, Albuquerque, NM, Email: vcalhoun@mrn.org
‡ Department of Electrical and Computer Engineering, University of New Mexico, Albuquerque, NM

***Abstract*—Joint analysis of neuroimaging data from multiple modalities has the potential to improve our understanding of brain function since each modality provides complementary information. In this paper, we address the problem of jointly analyzing functional magnetic resonance imaging (fMRI), structural MRI (sMRI) and electroencephalography (EEG) data collected during an auditory oddball (AOD) task with the goal of capturing neural patterns that differ between patients with schizophrenia and healthy controls. Traditionally, fusion methods such as joint independent component analysis (jICA) have been used to jointly analyze such multi-modal neuroimaging data. However, previous jICA analyses typically analyze the EEG signal from a single electrode or concatenate signals from multiple electrodes, thus ignoring the potential multilinear structure of the EEG data, and models the data using a common mixing matrix for both modalities. In this paper, we arrange the multi-channel EEG signals as a third-order tensor with modes: *subjects*, *time samples* and *electrodes*, and jointly analyze the tensor with the fMRI and sMRI data, both in the form of *subjects* by *voxels* matrices, using a structure-revealing coupled matrix and tensor factorization (CMTF) model. Through this modeling approach, we (i) exploit the multilinear structure of multi-channel EEG data and (ii) capture weights for components indicative of the level of contribution from each modality. We compare the results of the structure-revealing CMTF model with those of jICA and demonstrate that, while both models capture significant distinguishing patterns between patients and controls, the structure-revealing CMTF model provides more robust activation.**

I. Introduction

Different neuroimaging techniques provide complementary information about neural function/structure at different scales [1]. Therefore, joint analyses of signals from multiple neuroimaging modalities are of great interest to better understand neurological disorders [2], [3]. Functional modalities such as electroencephalography (EEG) and functional magnetic resonance imaging (fMRI) can be used to study the changes in neural activities triggered by an event in both patients affected by schizophrenia as well as healthy controls [2]. In addition to functional methods, anatomical neuroimaging techniques such as structural MRI (sMRI) can also capture structural differences between patients and controls [1], and since structure underlies function, joint analysis of these three modalities is expected to provide a more comprehensive picture.

The fusion of signals from multiple data sources is a challenging task due to the heterogeneity of the data from different sources. One type of heterogeneity is the order of the data, *e.g.*, while multi-channel EEG signals can be represented as a third-order tensor with modes: *subjects*, *time samples* and *electrodes*, fMRI and sMRI signals are often arranged as *subjects* by *voxels* matrices (Figure 1). The traditional approach used for jointly analyzing such neuroimaging data, first either matricizes the higher-order tensors [4] or selects a single EEG electrode [2], thus ignoring the potential multilinear structures of multi-channel EEG signals. Then these approaches use matrix factorization-based fusion methods such as joint independent component analysis (jICA) [5], linked ICA [6], parallel ICA [7] and transposed independent vector analysis (tIVA) [2]. However, matrix factorization-based fusion models need additional constraints such as orthogonality and independence to obtain a unique model, and may fail to capture the true factors due to those constraints [8].

In contrast, coupled matrix and tensor factorizations (CMTF) have recently proven useful for analyzing heterogeneous data sets jointly and without imposing strong constraints on the factors when the higher-order tensors have a defined multilinear structure [8]. In addition, through the exploration of the multilinear structure inherent to such data greater understanding of brain activity can be achieved [9], [10], [11]. Therefore, recent studies have arranged multi-channel EEG signals as higher-order tensors and used CMTF-type methods to fuse EEG and magnetoencephalography [12], EEG and gaze data [13] as well as EEG and fMRI [14], [3].

In this paper, with a goal of capturing patterns that differentiate patients with schizophrenia from healthy controls, we jointly analyze fMRI, sMRI and EEG data collected during an auditory oddball task. Multi-channel EEG signals are arranged as a third-order tensor, while fMRI and sMRI data are represented as matrices (Figure 1). To the best of our knowledge, the only other study that jointly analyzes EEG and fMRI signals coupled in the *subjects* mode using a CMTF model is by Hunyadi et al. [3], to study epileptic activities. The CMTF model used in [3] assumes that all extracted factors are shared by EEG and fMRI data. Rather than such a CMTF model, which may fail to provide a unique solution in the presence of both shared/unshared components [15], we use a structure-revealing CMTF model, known as the advanced CMTF (ACMTF) model [15], revealing the weights

ISBN 978-0-9928626-7-1

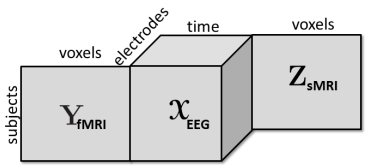

Fig. 1: A third-order tensor representing multi-channel EEG signals coupled with fMRI and sMRI data in the form of matrices in the *subjects* mode.

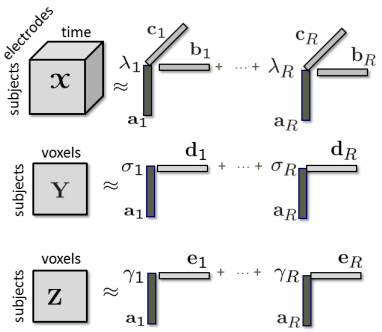

Fig. 2: Modeling of tensor $\mathcal{X}$ coupled with matrices $\mathbf{Y}$ and $\mathbf{Z}$ in the *subjects* mode using a structure-revealing CMTF model.

of components in each modality to identify shared/unshared factors and understand the contribution from each modality. Previously, we have shown the promise of the ACMTF model in a joint analysis of fMRI and multi-channel EEG data in terms of capturing neural patterns that can differentiate patients with schizophrenia from healthy controls [16]. Our contributions in this paper are: (i) In addition to fMRI and EEG, we also incorporate sMRI data into the ACMTF model and demonstrate that the model can capture spatial and temporal patterns that differ between patients and controls. (ii) We use the ACMTF model to demonstrate that the sMRI dataset contributes least to the model. (iii) We compare the results using the ACMTF model to those obtained using the popular fusion method jICA in terms of capturing patterns that differ between the two groups and show that the ACMTF model produces more robust results in terms of estimated differences.

II. Methodology

In this section, we briefly discuss the ACMTF and jICA models. Let the third-order tensor $\mathcal{X} \in \mathbb{R}^{I \times J \times K}$ with modes: *subjects*, *time samples* and *electrodes*, and matrices $\mathbf{Y} \in \mathbb{R}^{I \times M}$ (*subjects* by *voxels*) and $\mathbf{Z} \in \mathbb{R}^{I \times L}$ (*subjects* by *voxels*), represent the multi-channel EEG, fMRI and sMRI data, respectively.

A. Coupled Matrix/Tensor Factorizations

Given the third-order tensor $\mathcal{X}$ coupled with matrices $\mathbf{Y}$ and $\mathbf{Z}$ in the *subjects* mode, we can jointly factorize them using the ACMTF model that fits a CANDECOMP/PARAFAC (CP) model [17], [18] to tensor $\mathcal{X}$ and factorizes matrices $\mathbf{Y}$ and $\mathbf{Z}$ in such a way that the factor matrix extracted from the common, *i.e.*, *subjects*, mode is the same in the factorizations of all data sets. The R-component ACMTF model minimizes the following objective function:

$$
\begin{aligned}
&f(\boldsymbol{\lambda}, \boldsymbol{\Sigma}, \boldsymbol{\Gamma}, \mathbf{A}, \mathbf{B}, \mathbf{C}, \mathbf{D}, \mathbf{E}) \\
&= \| \mathcal{X} - [\![\boldsymbol{\lambda}; \mathbf{A}, \mathbf{B}, \mathbf{C}]\!] \|^2 + \| \mathbf{Y} - \mathbf{A}\boldsymbol{\Sigma}\mathbf{D}^{\mathsf{T}} \|^2 + \| \mathbf{Z} - \mathbf{A}\boldsymbol{\Gamma}\mathbf{E}^{\mathsf{T}} \|^2 \\
&\quad + \beta \| \boldsymbol{\lambda} \|_1 + \beta \| \boldsymbol{\sigma} \|_1 + \beta \| \boldsymbol{\gamma} \|_1 ,
\end{aligned} \tag{1}
$$

where the columns of factor matrices have unit norm, *i.e.*, $\| \mathbf{a}_r \| = \| \mathbf{b}_r \| = \| \mathbf{c}_r \| = \| \mathbf{d}_r \| = \| \mathbf{e}_r \| = 1$ for $r = 1, \ldots, R$. The CP model is denoted as $[\![\boldsymbol{\lambda}; \mathbf{A}, \mathbf{B}, \mathbf{C}]\!] = \sum_{r=1}^{R} \lambda_r \mathbf{a}_r \circ \mathbf{b}_r \circ \mathbf{c}_r$, where $\circ$ indicates the vector outer product, and $\mathbf{A} \in \mathbb{R}^{I \times R} = [\mathbf{a}_1 \ldots \mathbf{a}_R], \mathbf{B} \in \mathbb{R}^{J \times R} = [\mathbf{b}_1 \ldots \mathbf{b}_R], \mathbf{C} \in \mathbb{R}^{K \times R} = [\mathbf{c}_1 \ldots \mathbf{c}_R]$ correspond to factor matrices in the *subjects*, *time samples* and *electrodes* modes, respectively. $\boldsymbol{\lambda}, \boldsymbol{\sigma}, \boldsymbol{\gamma} \in \mathbb{R}^{R \times 1}$ are the weights of rank-one terms in $\mathcal{X}$, $\mathbf{Y}$, and $\mathbf{Z}$, respectively. $\boldsymbol{\Sigma}, \boldsymbol{\Gamma} \in \mathbb{R}^{R \times R}$ are diagonal matrices with entries of $\boldsymbol{\sigma}$ and $\boldsymbol{\gamma}$ on the diagonal. $\mathbf{D} \in \mathbb{R}^{M \times R}$ and $\mathbf{E} \in \mathbb{R}^{L \times R}$ correspond to factor matrices in the *voxels* mode in fMRI and sMRI, respectively. $\| \, . \, \|$ denotes the Frobenius norm for matrices/higher-order tensors, and the 2-norm for vectors. $\| \, . \, \|_1$ denotes the 1-norm of a vector, *i.e.*, $\| \mathbf{x} \|_1 = \sum_{r=1}^{R} |x_r|$, and $\beta > 0$ is a penalty parameter. Imposing penalties on the weights in (1) sparsifies the weights so that unshared factors have weights close to 0 in some data sets. The model is illustrated in Figure 2.

By modeling $\mathcal{X}$ using a CP model, we assume that component r models a brain activity with temporal and spatial patterns represented by $\mathbf{b}_r$ and $\mathbf{c}_r$, respectively. Multi-channel EEG signals from each subject are a linear mixture of these R brain activities mixed using subject-specific weights. Also, by jointly analyzing neuroimaging data using the ACMTF model, we assume that each component extracted from $\mathcal{X}$ models a brain activity with certain temporal ($\mathbf{b}_r$) and spatial ($\mathbf{c}_r$) signatures, and the corresponding component in $\mathbf{Y}$ models that brain activity with higher spatial specificity using $\mathbf{d}_r$, while the component in $\mathbf{Z}$ provides information about the tissue type at a very high spatial resolution using $\mathbf{e}_r$. Since the same factor matrix, $\mathbf{A}$, is extracted from the *subjects* mode of all data sets, subject covariations in all modalities are assumed to be the same. Note that the significance of the components can be assessed using a two-sample *t*-test on each column of $\mathbf{A}$, where the first group is the coefficients corresponding to healthy controls and the second group is the coefficients corresponding to patients. The CP model is unique under mild conditions [19] and the ACMTF inherits uniqueness properties from CP [20]. In the presence of both shared/unshared components, 1-norm penalties on the weights help to obtain unique solutions [15].

B. JICA

An alternative approach to jointly analyze $\mathcal{X}$, $\mathbf{Y}$ and $\mathbf{Z}$ is to use a matrix factorization-based fusion approach by matricizing $\mathcal{X}$ in the *subjects* mode as a *subjects* by *time samples* $\times$ *electrodes* matrix, denoted as $\mathbf{X}_{(1)}$.

ISBN 978-0-9928626-7-1 © EURASIP 2017

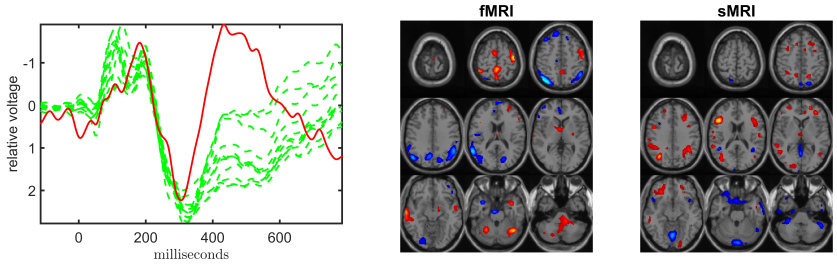

(a) Component 1 with p-value: 6.1×10^{-3}

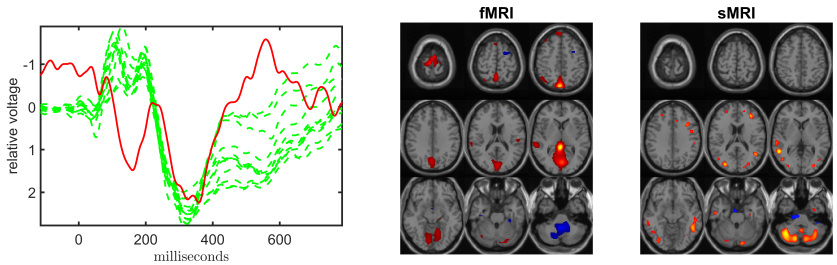

(b) Component 3 with p-value: 4.9×10^{-3}

Fig. 3: Components from ACMTF that remain significant after a Bonferroni correction, $p < 0.005$. Reported p-values are not corrected for multiple comparisons. $\mathbf{b}_r$, $\mathbf{d}_r$ and $\mathbf{e}_r$ corresponding to the *time samples* mode in EEG and *voxels* modes in fMRI and sMRI are plotted. For EEG plots, $\mathbf{b}_r$ is plotted in red while green dashed plots show signals from individual electrodes averaged across all subjects. The fMRI and sMRI plots are z-maps, thresholded at $z = 2.7$, where red indicates an increase in controls over patients and blue indicates an increase in patients over controls.

JICA concatenates matrices representing the data from different modalities and models the constructed matrix using an ICA model as follows:

$$[\mathbf{X}_{(1)} \ \mathbf{Y} \ \mathbf{Z}] = \mathbf{AS} \tag{2}$$

where, for an R-component ICA model, $\mathbf{A} \in \mathbb{R}^{I \times R}$ corresponds to the mixing matrix, similar to the factor matrix in (1), and $\mathbf{S} \in \mathbb{R}^{R \times (JK+M+L)}$ represents the source signals. Note that the subject covariations across all data sets, *i.e.*, modalities, are assumed to be the same in jICA as in ACMTF, since the same mixing matrix is shared across the datasets. However, in this case the model does not include an adaptive estimation of contributions from each modality as in ACMTF. The rows of $\mathbf{S}$ correspond to patterns of brain activity and are assumed to be statistically independent.

In the next section, we compare ACMTF and jICA in terms of their ability to extract meaningful patterns that differ between patients with schizophrenia and healthy controls.

III. Experiments

A. Data

The EEG, fMRI and sMRI data were separately collected from 21 healthy controls and 11 patients with schizophrenia during an auditory oddball task, where subjects pressed a button when they detected an infrequent target sound within a series of auditory stimuli. For the fMRI data, we computed task-related spatial activity maps for each subject, calculated by the general linear model-based regression approach using the statistical parametric mapping toolbox [21]. By making use of these features, we constructed a matrix of 32 *subjects* by 60186 *voxels* representing the fMRI signals. For the EEG data, for each electrode, we averaged small windows around the target tone across the repeated instances, deriving event-related potentials. Out of 64 electrodes in total, we used multiple electrodes from the frontal, motor and parietal areas, *i.e.*, AF3, AF4, Fz, T7, C3, Cz, C4, T8, Pz, PO3 and PO, based on our previous results [16], which demonstrate better interpretability using this subset rather than all electrodes. Multi-channel EEG signals were then arranged as a third-order tensor: 32 *subjects* by 451 *time samples* by 11 *electrodes*. For the sMRI data, we computed probabilistically segmented gray matter images for each subject and by using these features formed a matrix of 32 *subjects* by 306640 *voxels*. For more details, see [2].

B. Experimental Setting

Before the analysis, we mean-centered the third-order EEG tensor across the *time* mode, and scaled within the *subjects* mode by dividing each horizontal slice by its standard deviation. The fMRI and sMRI data were also preprocessed by mean-centering each row and dividing each row by its standard deviation. For both models, the data sets were preprocessed in nearly the same way. The steps in which they differ are: (i) in jICA, (before preprocessing) the EEG data was repeated ten times resulting in a third-order tensor of size $32 \times 4510 \times 11$ to make the number of samples approximately the same order as the fMRI and sMRI data after unfolding, (ii) in structure-revealing CMTF, (after preprocessing) each data set was divided by its Frobenius norm to give equal importance to the approximation of each data set in (1).

In order to fit the ACMTF model, we use ACMTF-OPT [15] from the CMTF Toolbox and the nonlinear conjugate gradient

ISBN 978-0-9928626-7-1 © EURASIP 2017

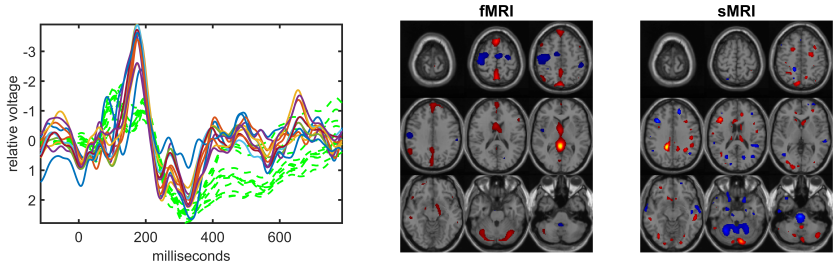

(a) Component with p-value: 7.0×10^{-4}

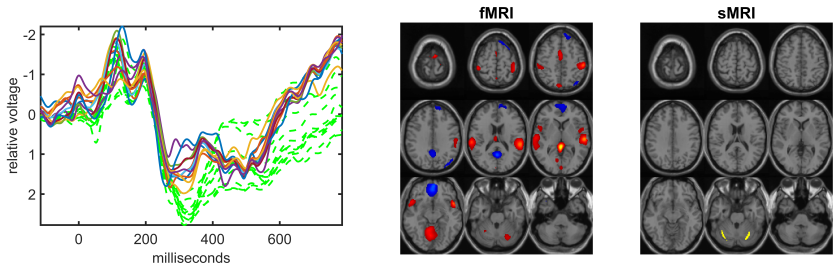

(b) Component with p-value: 3.6×10^{-3}

Fig. 4: Components from jICA that remain significant after a Bonferroni correction, $p < 0.005$. Reported p-values are not corrected for multiple comparisons. Parts of $\mathbf{s}_r$ corresponding to the *time samples* for each electrode in EEG and *voxels* in fMRI and sMRI are plotted. In EEG plots, green dashed plots show signals from individual electrodes averaged across all subjects. The fMRI and sMRI plots are z-maps, thresholded at $z = 2.7$, where red indicates an increase in controls over patients and blue indicates an increase in patients over controls.

algorithm from the Poblano Toolbox. The penalty parameter is set to $\beta = 10^{-3}$. A number of random initializations are used and, after making sure that the model is unique, the solution corresponding to the minimum function value is reported.

For jICA, we unfold the preprocessed EEG tensor in the *subjects* mode and concatenate the resulting matrix with fMRI and sMRI matrices. The concatenated matrix is modeled using an ICA algorithm based on entropy bound minimization [22], which makes use of a flexible density model, since the richer data distribution encountered as a result of concatenation benefits from such flexibility [2]. We fit the model using a number of initializations and report the most stable run determined by a minimum spanning tree-based approach [23].

The number of components, R, is empirically chosen to be 10 for both models. Note that the optimal R may be different for the two models. In order to probe this, for ACMTF, we increased R up to 15 and found that increasing R introduced components with small weights, *i.e.*, < 0.1, in sMRI and made it difficult to get a unique solution. For jICA, we observed similar significant components for $R = 15$. An extensive study on order selection is a topic of future research.

C. Results

As shown in Figures 3 and 4, both ACMTF and jICA captured significant components that can differentiate between patients and controls.

Out of the 10 components found by ACMTF, Figure 3 displays the components, 1 and 3, with statistically significant p-values that survive the Bonferroni correction. The first component, shown in Figure 3(a), whose EEG corresponds to the N2-P3 transition, shows higher motor activation for the controls over the patients and higher parietal activation in the patients over the controls. For this component, from the sMRI, we note that there is an increased concentration of gray matter throughout the parietal lobe for controls over patients and a decrease in concentration of gray matter in certain sections of the cerebellum for controls versus patients. This component is very similar to a component found using only the fMRI and EEG data [16]; however, we note that the structure of the default mode network (DMN) activation shown in the fMRI plot is much clearer when only the fMRI and EEG data are analyzed. The second component, displayed in Figure 3(b), whose EEG component describes the P2 and P3 peaks, shows higher fMRI activation in the superior parietal cortex and the visual cortex for the patients over the controls. This component is nearly identical to a component found when only the fMRI and EEG data were analyzed [16]. However, from this joint analysis we find that this component is associated with an increase in concentration of gray matter in controls over patients in sections of the parietal lobe and cerebellum. We should note that the significance of both components is lower in this study than it was in joint analysis of only fMRI and EEG. This fact has previously been noted [2] and combined with the fact that weights of the rank-one terms in sMRI are almost always lower than the ones in fMRI and EEG, as shown in Figure 5, seems to imply that the sMRI data contributes less to the results and is itself less discriminative than the fMRI and EEG data. This observation correlates with the result found in [24], which also showed a weaker contribution from the sMRI.

Similarly, as shown in Figure 4, jICA also captures two components with statistically significant p-values that survive

ISBN 978-0-9928626-7-1

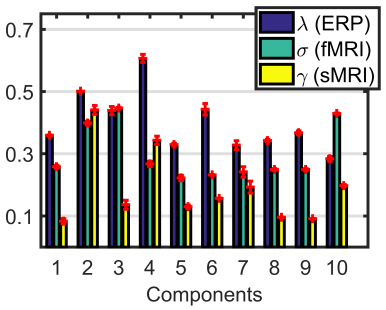

Fig. 5: Weights of the rank-one components in EEG, fMRI and sMRI extracted using a 10-component ACMTF model (for several runs returning the same function value, and error bars in red show the change in weights in different runs).

the Bonferroni correction. The first component, shown in Figure 4(a), whose EEG component describes the N2 peak, shows higher fMRI activation in the superior parietal cortex for the patients over the controls. The sMRI portion of this component shows both increased as well as decreased concentrations of gray matter for controls versus patients in the cerebellum. This component shows some similarities, especially in the fMRI and parts of the EEG with component 3 in ACMTF. The second significant component found using jICA, displayed in Figure 4(b), whose EEG component describes the N1, P2, N2 peaks and the N2-P3 transition, shows increased fMRI activation in the motor cortex and temporal lobe for the controls versus the patients. This component also shows increased gray matter concentration in the cerebellum in controls versus patients. This component shares similarities with a component found in a jICA analysis of similar data where only the Cz channel was analyzed [2].

IV. Conclusion

In this paper, we have addressed the problem of jointly analyzing neuroimaging data from multiple modalities using the ACMTF model. This model enables the processing of multi-channel EEG signals as third-order tensors and the determination of the relative contribution from each modality. We compared the ACMTF model with the popular fusion method, jICA. Our results on joint analysis of EEG, fMRI and sMRI demonstrates that, while both jICA and the ACMTF model capture meaningful distinguishing patterns between patients with schizophrenia and healthy controls, ACMTF, with its less restrictive model that estimates contribution of each modality, captures more robust regions of activation, particularly in the sMRI data.

These promising results motivate a more comprehensive comparison of CMTF-based approaches with jICA and more general fusion methods, such as tIVA, promising to elucidate the comparative advantages and limitations of all these fusion methods.

Acknowledgment

This work was funded by the Danish Council for Independent Research under the projects 11-116328 and 11-120947 as well as NSF-CCF 1618551 and NIH R01 EB 005846 grants.

References

[1] S. A. Bunge and I. Kahn, "Cognition: An overview of neuroimaging techniques," *Encyc. of Neuroscience*, vol. 2, pp. 1063–1067, 2009.
[2] T. Adalı, Y. Levin-Schwartz, and V. D. Calhoun, "Multimodal data fusion using source separation: Application to medical imaging," *Proceedings of the IEEE*, vol. 103, pp. 1494–1506, 2015.
[3] B. Hunyadi, W. V. Paesschen, M. De Vos, and S. Van Huffel, "Fusion of electroencephalography and functional magnetic resonance imaging to explore epileptic network activity," in *EUSIPCO*, 2016, pp. 240–244.
[4] W. Swinnen, B. Hunyadi, E. Acar, S. Van Huffel, and M. De Vos, "Incorporating higher dimensionality in joint decomposition of EEG and fMRI," in *EUSIPCO*, 2014, pp. 121–125.
[5] V. D. Calhoun, T. Adalı, G. D. Pearlson, and K. A. Kiehl, "Neuronal chronometry of target detection: Fusion of hemodynamic and event-related potential data," *NeuroImage*, vol. 30, pp. 544–553, 2006.
[6] A. R. Groves, C. F. Beckmann, S. M. Smith, and M. W. Woolrich, "Linked independent component analysis for multimodal data fusion," *NeuroImage*, vol. 54, pp. 2198–2217, 2011.
[7] V. D. Calhoun, J. Liu, and T. Adalı, "A review of group ICA for fMRI data and ICA for joint inference of imaging, genetic, and ERP data," *NeuroImage*, vol. 45, pp. S163–S172, 2009.
[8] E. Acar, R. Bro, and A. K. Smilde, "Data fusion in metabolomics using coupled matrix and tensor factorizations," *Proceedings of the IEEE*, vol. 103, pp. 1602–1620, 2015.
[9] J. Möcks, "Topographic components model for event-related potentials and some biophysical considerations," *IEEE Trans. on Biomed. Eng.*, vol. 35, pp. 482–484, 1988.
[10] E. Acar, C. A. Bingol, H. Bingol, R. Bro, and B. Yener, "Multiway analysis of epilepsy tensors," *Bioinformatics*, vol. 23, no. 13, pp. i10–i18, 2007.
[11] M. Mørup, L. K. Hansen, and S. M. Arnfred, "ERPWAVELAB a toolbox for multi-channel analysis of time - frequency transformed event related potentials," *J. Neurosci. Methods*, vol. 161, pp. 361–368, 2007.
[12] H. Becker, P. Comon, and L. Albera, "Tensor-based processing of combined EEG/MEG data," in *EUSIPCO*, 2012, pp. 275–279.
[13] B. Rivet, M. Duda, A. Guerin-Dugue, C. Jutten, and P. Comon, "Multimodal approach to estimate the ocular movements during EEG recordings: a coupled tensor factorization method," in *EMBC*, 2015.
[14] E. Karahan, P. Rojas-Lopez, M. Bringas-Vega, P. Valdes-Hernandez, and P. A. Valdes-Sosa, "Tensor analysis and fusion of multimodal brain images," *Proceedings of the IEEE*, vol. 103, pp. 1531–1559, 2015.
[15] E. Acar, E. E. Papalexakis, G. Gurdeniz, M. A. Rasmussen, A. J. Lawaetz, M. Nilsson, and R. Bro, "Structure-revealing data fusion," *BMC Bioinformatics*, vol. 15, p. 239, 2014.
[16] E. Acar, Y. Levin-Schwartz, V. D. Calhoun, and T. Adalı, "Tensor-based fusion of EEG and FMRI to understand neurological changes in schizophrenia," in *ISCAS*, 2017, pp. 314–317.
[17] R. A. Harshman, "Foundations of the PARAFAC procedure: Models and conditions for an "explanatory" multi-modal factor analysis," *UCLA Working Papers in Phonetics*, vol. 16, pp. 1–84, 1970.
[18] J. D. Carroll and J.-J. Chang, "Analysis of individual differences in multidimensional scaling via an N-way generalization of "Eckart-Young" decomposition," *Psychometrika*, vol. 35, pp. 283–319, 1970.
[19] T. G. Kolda and B. W. Bader, "Tensor decompositions and applications," *SIAM Review*, vol. 51, no. 3, pp. 455–500, 2009.
[20] M. Sorensen and L. De Lathauwer, "Coupled canonical polyadic decompositions and (coupled) decompositions in multilinear rank-$(l_{r,n}, l_{r,n}, 1)$ terms — part i: Uniqueness," *SIMAX*, vol. 36, pp. 496–522, 2015.
[21] K. Friston. (2013, Jan.) SPM. [Online]. Available: http://www.fil.ion.ucl.ac.uk/spm/software/spm8
[22] X.-L. Li and T. Adalı, "Independent component analysis by entropy bound minimization," *IEEE Trans. Signal Process.*, vol. 58, no. 10, pp. 5151–5164, 2010.
[23] W. Du, Y. Levin-Schwartz, G. D. Fu, S. Ma, V. D. Calhoun, and T. Adalı, "The role of diversity in complex ICA algorithms for fMRI analysis," *J. Neurosci. Methods*, vol. 264, pp. 129–135, 2016.
[24] Y. Levin-Schwartz, Y. Song, P. J. Schreier, V. D. Calhoun, and T. Adalı, "Sample-poor estimation of order and common signal subspace with application to fusion of medical imaging data," *NeuroImage*, vol. 134, pp. 486–493, 2016.

ISBN 978-0-9928626-7-1 © EURASIP 2017